Electronic Supplementary Material (ESI) for Journal of Materials Chemistry B.
This journal is © The Royal Society of Chemistry 2022

SUPPORTING INFORMATION

Unexpected Luminescence of Non-conjugated Biomass-Based Polymers: New Approach in Photothermal Imaging

Felipe de la Cruz-Martínez,[a,≠] Roger Bresolí-Obach,[b,c,≠] Iván Bravo,[d] Carlos Alonso-Moreno,[e] Daniel Hermida-Merino,[f] Johan Hofkens,[b] Agustín Lara-Sánchez,[*,a] José A. Castro-Osma,[*,e] Cristina Martín[*,b,d]

Abstract: Population growth, world resources depletion and persistent toxic chemical production underline the need to seek new smart materials from inexpensive, biodegradable, and renewable feedstocks. Hence, “metal-free” ring-opening copolymerization to convert biomass carvone-based monomers into non-conventional luminescent biopolymers is considered a sustainable approach to achieve these goals. The non-conventional emission was studied in terms of steady-state and time-resolved spectroscopy in order to unravel the structure-properties for different carvone-based copolymers. The results highlighted the importance of the final copolymer folding structure as well as its environment in luminescent behavior (cluster-triggered emission). In all cases, their luminescent behavior is sensitive to small temperature fluctuations (where the minimum detected temperature is T_m ~ 2 ºC and relative sensitivity is S_r ~ 6 % $ºC^{-1}$) even at the microscopic scale, which endows these materials a great potential as thermosensitive smart polymers for photothermal imaging.

Table of Contents

Materials and methods S1

Table S1. Synthesis of carvone-derived biopolyesters using DMAP as catalyst S2

Figure S1. ^{1}H NMR spectrum of poly(PA-*alt*-COendo) (**1**) S3

Figure S2. $^{13}C\{^{1}H\}$ NMR spectrum of poly(PA-*alt*-COendo) (**1**) S3

Figure S3. IR spectrum of poly(PA-*alt*-COendo) (**1**) S4

Figure S4. GPC profile of poly(PA-*alt*-COendo) (**1**) S4

Figure S5. TGA analysis of poly(PA-*alt*-COendo) (**1**) S5

Figure S6. DSC analysis of poly(PA-*alt*-COendo) (**1**) S5

Figure S7. ^{1}H NMR spectrum of poly(SA-*alt*-COendo) (**2**) S6

Figure S8. $^{13}C\{^{1}H\}$ NMR spectrum of poly(SA-*alt*-COendo) (**2**) S6

Figure S9. IR spectrum of poly(SA-*alt*-COendo) (**2**) S7

Figure S10. GPC profile of poly(SA-*alt*-COendo) (**2**) S7

Figure S11. TGA analysis of poly(SA-*alt*-COendo) (**2**) S8

Figure S12. DSC analysis of poly(SA-*alt*-COendo) (**2**) S8

Figure S13. ^{1}H NMR spectrum of poly(PA-*alt*-COexo) (**3**) S9

Figure S14. $^{13}C\{^{1}H\}$ NMR spectrum of poly(PA-*alt*-COexo) (**3**) S9

Figure S15. IR spectrum of poly(PA-*alt*-COexo) (**3**) S10

Figure S16. GPC profile of poly(PA-*alt*-COexo) (**3**) S10

Figure S17. TGA analysis of poly(PA-*alt*-COexo) (**3**) S11

Figure S18. DSC analysis of poly(PA-*alt*-COexo) (**3**) S11

Figure S19. ^{1}H NMR spectrum of poly(SA-*alt*-COexo) (**4**) S12

Figure S20. $^{13}C\{^{1}H\}$ NMR spectrum of poly(SA-*alt*-COexo) (**4**) S12

Figure S21. IR spectrum of poly(SA-*alt*-COexo) (**4**) S13

Figure S22. GPC profile of poly(SA-*alt*-COexo) (**4**) S13

Figure S23. TGA analysis of poly(SA-*alt*-COexo) (**4**) S14

Figure S24. DSC analysis of poly(SA-*alt*-COexo) (**4**) S14

Table S2. Spectroscopic and Temperature Analysis values for each polymer in different environments at the same concentration (10^{-4} M) S15

Figure S25. UV-visible spectra of polymers **1**-**4** at 10^{-4} M in different solvents S16

Figure S26. Emission spectra of polymers **1**-**4** at 10^{-4} M in different solvents upon excitation **A)** 290 nm and **B)** 340 nm S17

Figure S27: Photographic images of 3 ($1x10^{-4}$ M) dissolved in water, DMSO in daylight (left) and in the darkness (right) upon irradiation at violet (405 nm; top) and green light laser (532 nm; bottom). S18

Figure S28. Emission spectra of polymers **1-4** in THF/H_2O mixtures from 0 (black line) to 80% wt water fraction S19

Figure S29. UV-visible spectra (solid line) and emission spectra (dashed line) upon excitation at 360 nm of polymers **1-4** in solid state S20

Figure S30. Emission spectra of each polymer recorded at 20°C and 100 °C subjected to 10 repeated heating-cooling cycles in solid state S21

Figure S31. Dependence of **A)** WAXS and **B)** SAXS profiles of polymer 3 in solid state S22

Figure S32. Emission spectra upon excitation at 360 nm of each polymer in **A)** TOL, **B)** DMSO, **C)** EtOH and **D)** THF-WATER solution as a function of temperature (10 - 80ºC) S23

Figure S33. Correlation between change in intensity (F-F_0)/F vs sample temperature, showing a linear response in all polymers and solvents S24

Figure S34. A representative transmission image of the Au NPs dropped cast onto the coverslip surface. S25

Materials and methods

All polymerizations were performed under nitrogen, using standard Schlenk techniques. ^{1}H and ^{13}C NMR spectra were recorded on a Bruker Ascend TM-500 spectrometer and referenced to the residual deuterated solvent. Gel permeation chromatography (GPC) measurements were performed on a Shimadzu LC-20A instrument equipped with a TSK-GEL G3000H column and a refractive index detector (RID-20A). The GPC column was eluted with THF at 25 °C at 1 $mL \cdot min^{-1}$ and was calibrated using eight monodisperse polystyrene standards in the range 580–48300 Da. TGA analysis was performed on a TA instrument TGA-Q50. The heating rate for the sample was 10 °C/min, and the nitrogen flow rate was 60 mL/min. DSC curves were obtained under N_2 atmosphere on a TA Instrument DSC-Q20. Samples were weighed into aluminum crucibles with 5 mg of sample and subjected to two heating cycles at a heating rate of 10 °C/min.

All the solvents used were spectroscopic grade and purchased from Sigma Aldrich. Toluene used for copolymerization processes was predried over sodium wire and distilled under nitrogen from sodium. Deuterated solvents were stored over activated 4 Å molecular sieves and degassed by several freeze-thaw cycles. Carvone-based epoxides were pre-dried over calcium hydride, distilled under vacuum and stored under nitrogen in a glove box. Phthalic and succinic anhydride (Sigma-Aldrich) were sublimed three times and stored under nitrogen in a glove box. All other reagents were purchased from common commercial sources and used as received. The used Au nanospheres suspension with a nominal diameter of 200 nm (EM.GC200) was purchased to BBI solutions (Kent, UK).

Table S1. Synthesis of carvone-derived biopolyesters using DMAP as catalyst.[a]

Entry	Anhydride	Epoxide	t (h)	Conv.[b] (%)	TOF (h^{-1})[c]	Alternating degree[b] (%)	M_n (kDa) (PDI)[d]
1	PA	COEndo	48	88	0.37	>99	2.76 (1.91)
2	SA	COEndo	48	>99	0.40	>99	2.39 (1.83)
3	PA	COExo	24	92	0.77	>99	3.58 (1.64)
4	SA	COExo	24	>99	0.83	>99	3.12 (1.63)

[a]Reactions were carried out in toluene at 95 ºC with a molar ratio DMAP/anhydride/epoxide = 5:100:100. [b]Determined by ^{1}H NMR spectroscopy. [c]TOF = turnover frequency. [d]Determined by GPC analysis. Conversion of cyclic anhydrides was determined by ^{1}H NMR spectroscopy by relative integration of protons in PA ($CDCl_3$, δ = 7.8-8.0 ppm) or SA ($CDCl_3$, δ = 2.9 ppm) and poly(PA-*alt*-COEndo) ($CDCl_3$, δ = 7.5-7.8 ppm), poly(SA-*alt*-COEndo) ($CDCl_3$, δ = 2.5-2.8 ppm) or poly(PA-*alt*-COExo) ($CDCl_3$, δ = 7.4-7.8 ppm), poly(SA-*alt*-COExo) ($CDCl_3$, δ = 2.5-2.8 ppm).

The renewable carvone-derived polyesters were synthetized by ROCOP of phthalic or succinic anhydrides and carvone-based epoxides using DMAP as catalyst (Table 1). Reactions were carried out in toluene at 95ºC with a molar ratio 5:100:100 of DMAP, cyclic anhydride and epoxide. When carvone-derived *endo*-epoxide (COEndo) was used as monomer, copolymerizations required a longer time, which is attributable to the lower reactivity of tri-substituted epoxides compared with *gem*-di-substituted analogues (Table 1). On the other hand, ROCOP proceeded efficiently, and excellent conversions were obtained when succinic anhydride was used as substrate (Table 1, entries 2 and 4).

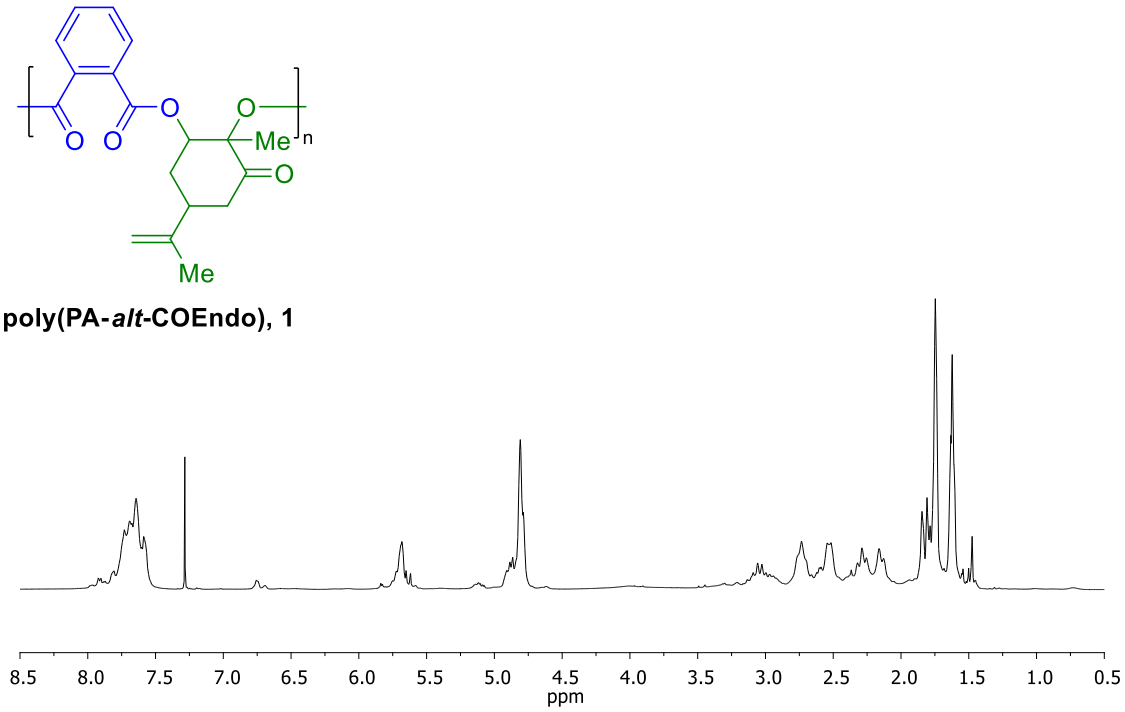

Figure S1. ^{1}H NMR spectrum of poly(PA-*alt*-COendo) (**1**)

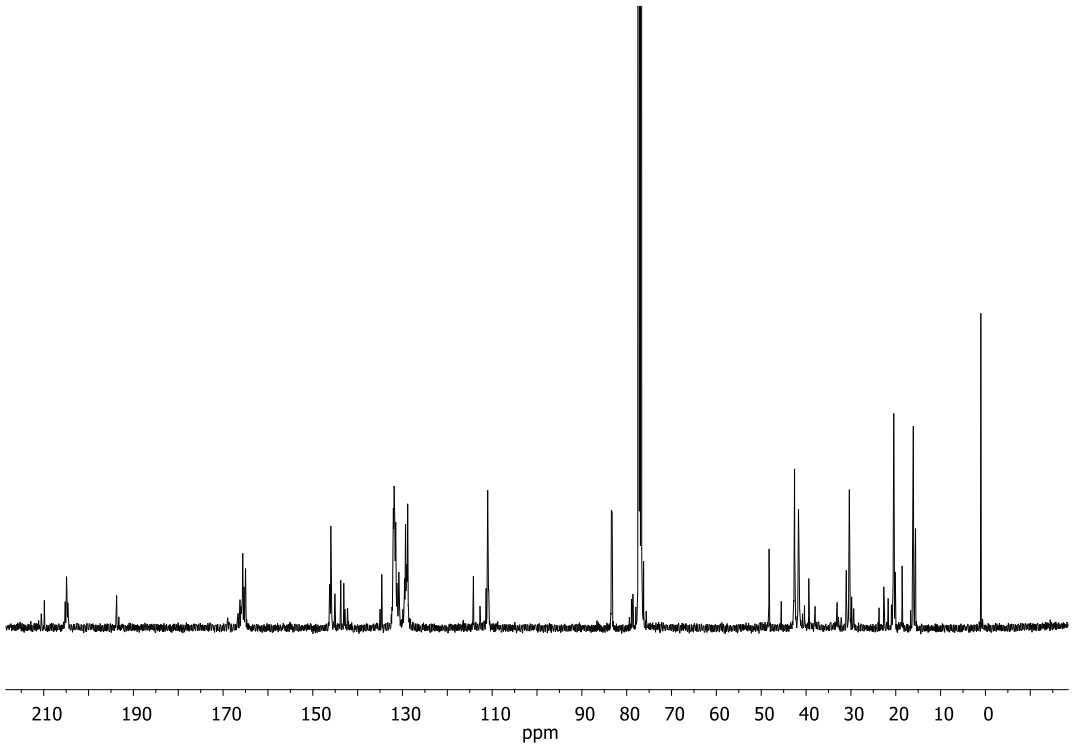

Figure S2. ^{13}C{^{1}H} NMR spectrum of poly(PA-*alt*-COendo) (**1**)

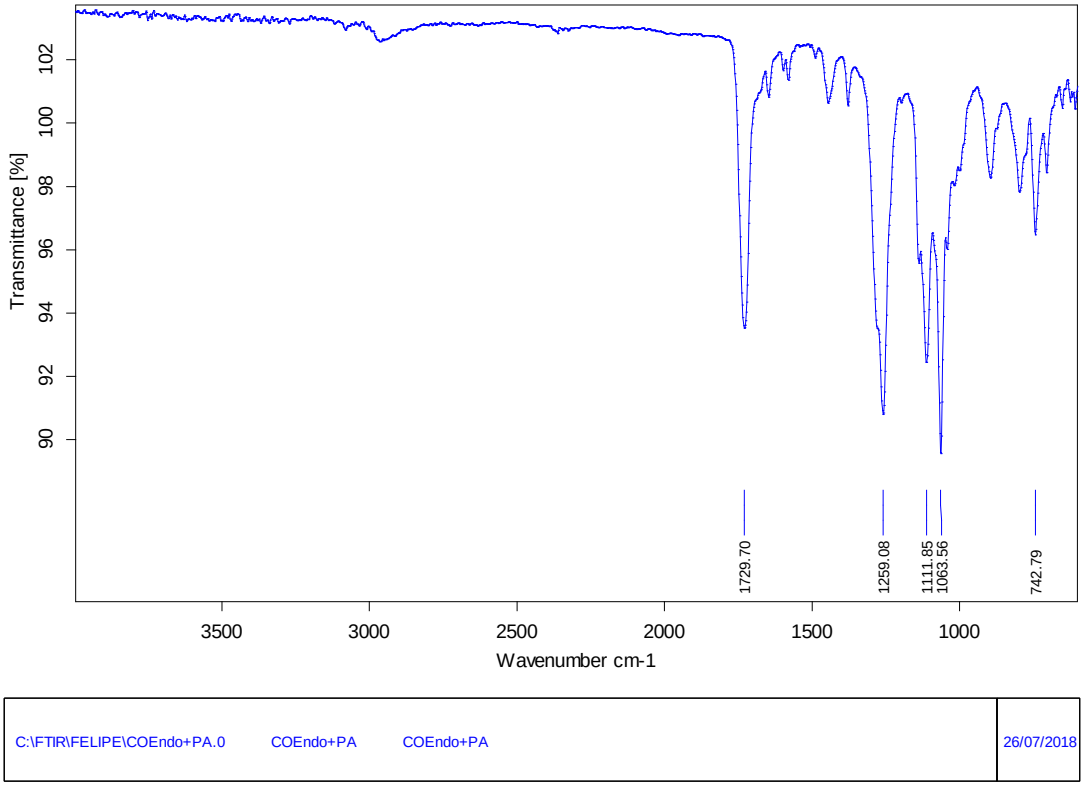

Figure S3. IR spectrum of poly(PA-*alt*-COendo) (**1**)

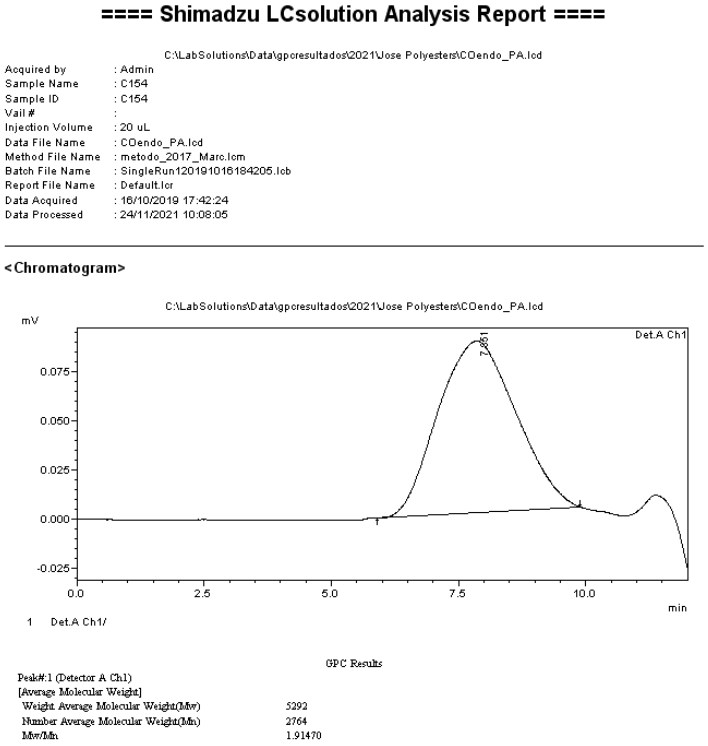

Figure S4. GPC profile of poly(PA-*alt*-COendo) (**1**)

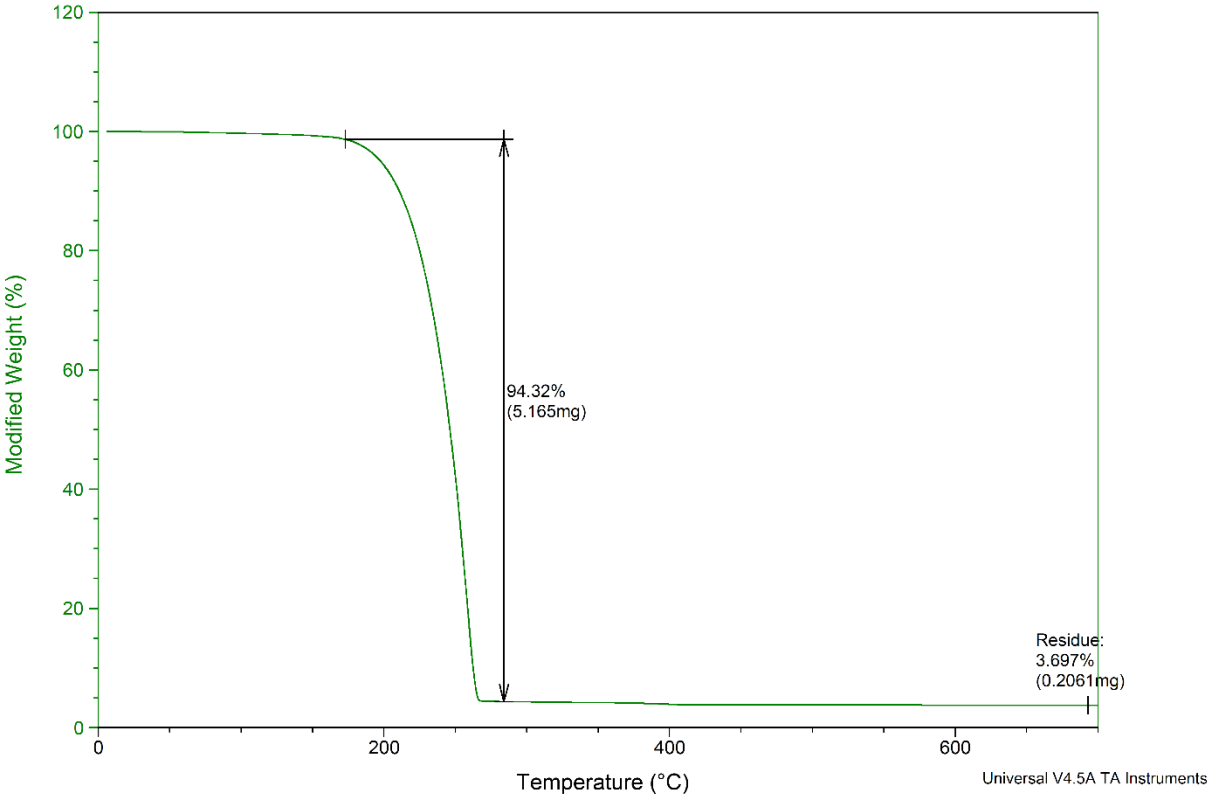

Figure S5. TGA analysis of poly(PA-*alt*-COendo) (**1**)

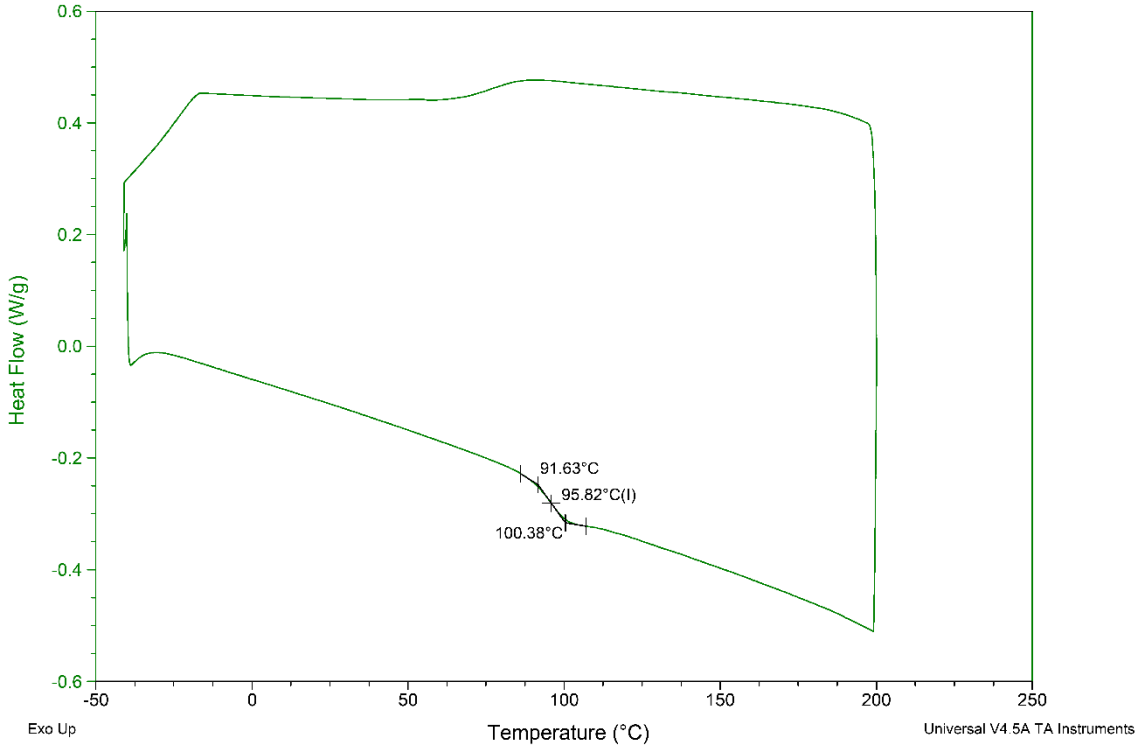

Figure S6. DSC analysis of poly(PA-*alt*-COendo) (**1**)

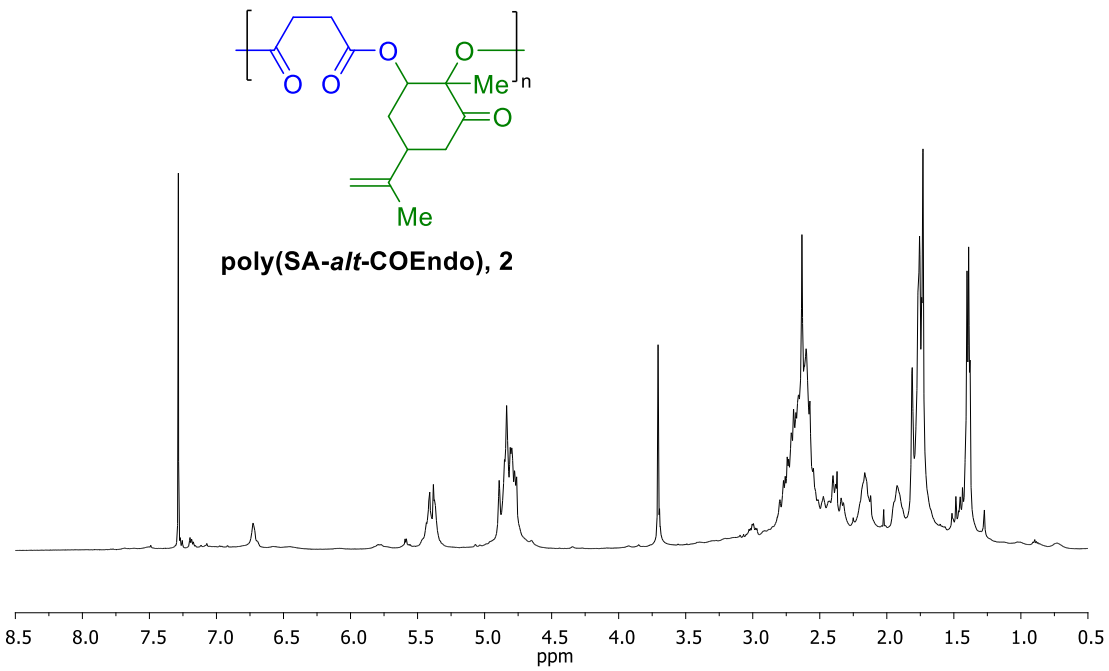

Figure S7. ^{1}H NMR spectrum of poly(SA-*alt*-COendo) (**2**)

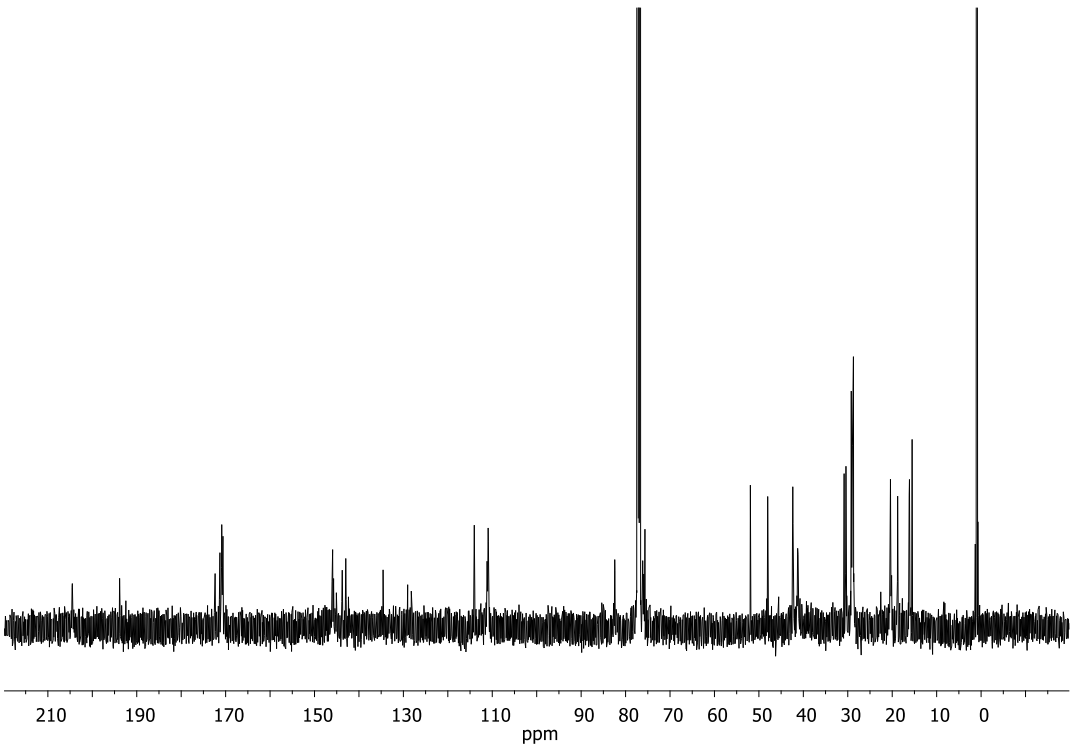

Figure S8. ^{13}C{^{1}H} NMR spectrum of poly(SA-*alt*-COendo) (**2**)

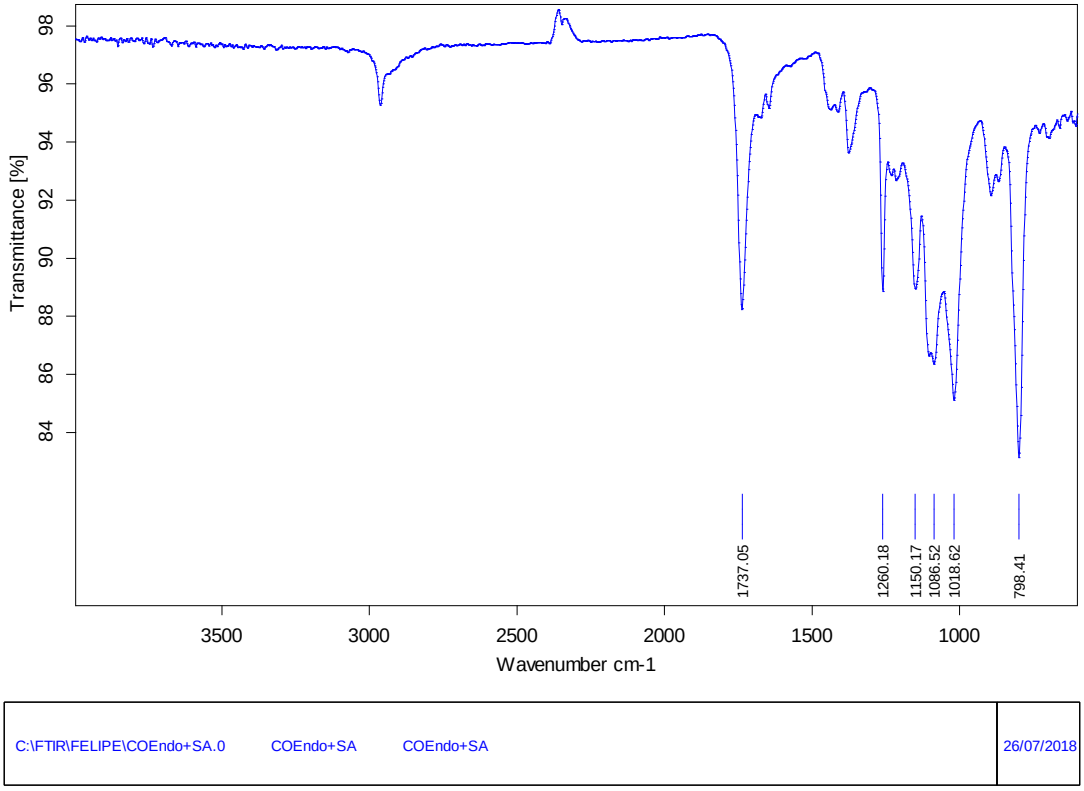

Figure S9. IR spectrum of poly(SA-*alt*-COendo) (**2**)

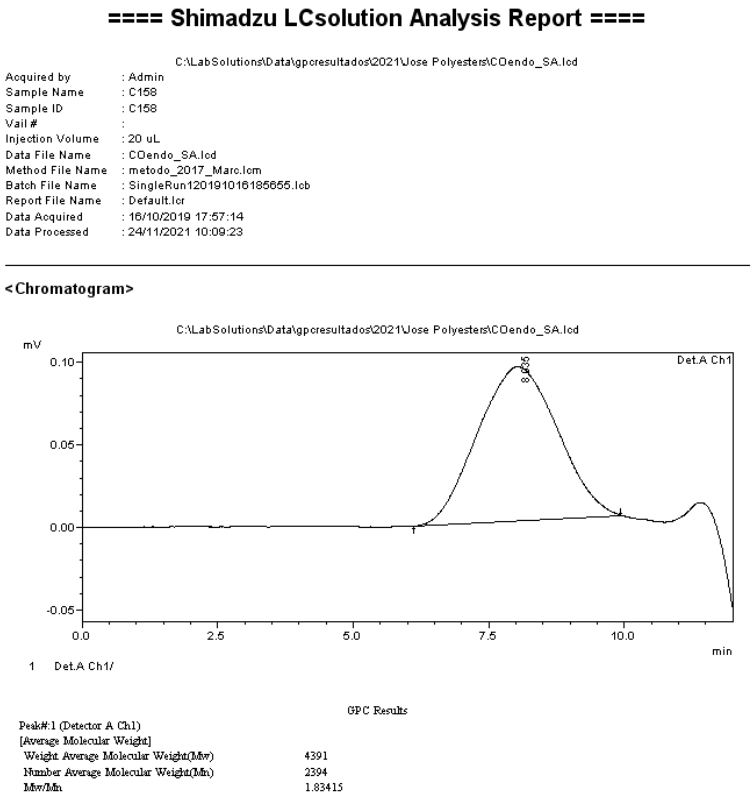

Figure S10. GPC profile of poly(SA-*alt*-COendo) (**2**)

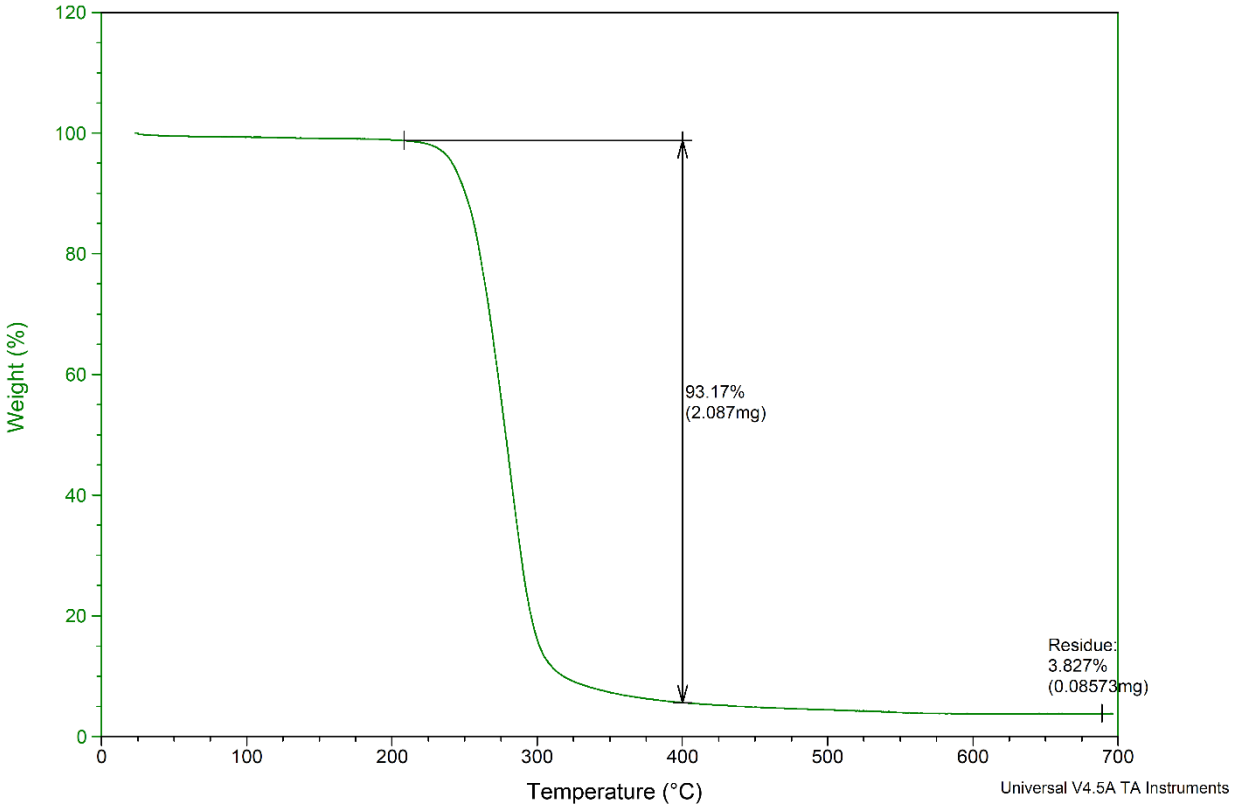

Figure S11. TGA analysis of poly(SA-*alt*-COendo) (**2**)

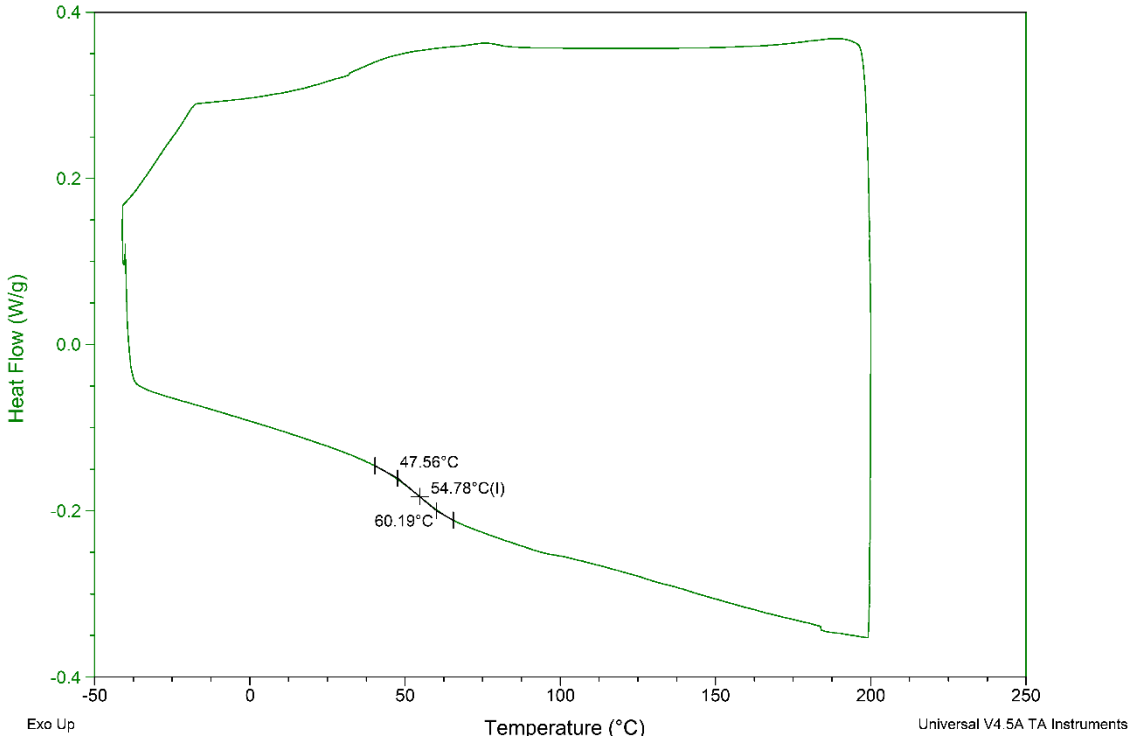

Figure S12. DSC analysis of poly(SA-*alt*-COendo) (**2**)

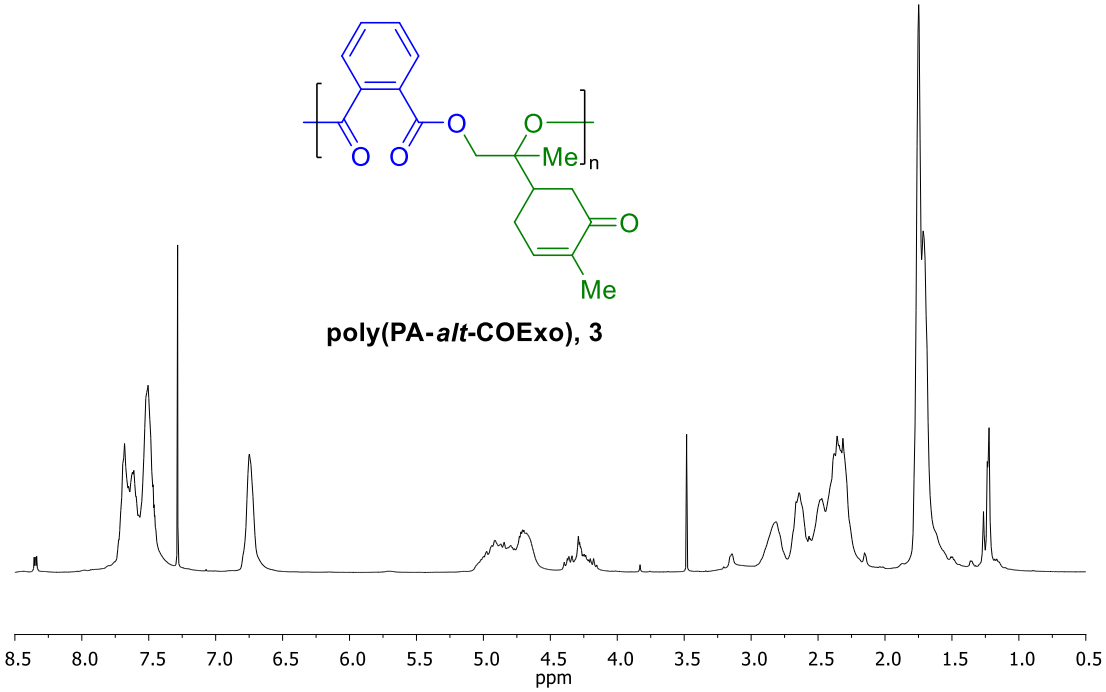

Figure S13. ^{1}H NMR spectrum of poly(PA-*alt*-COexo) (**3**)

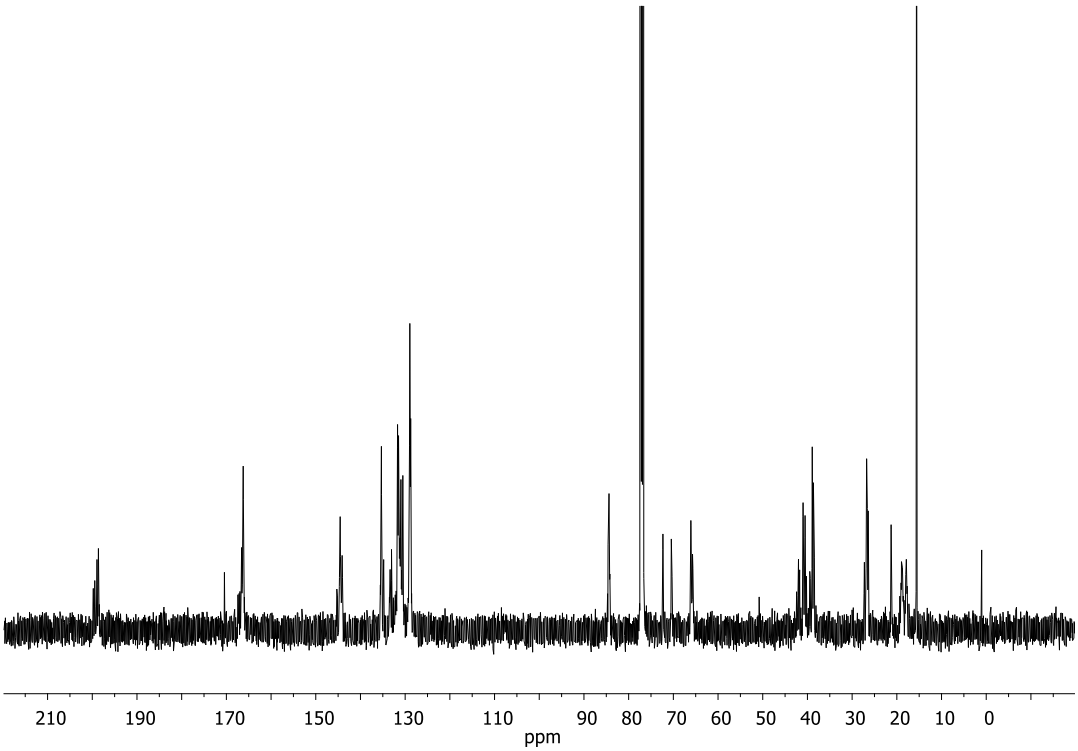

Figure S14. ^{13}C{^{1}H} NMR spectrum of poly(PA-*alt*-COexo) (**3**)

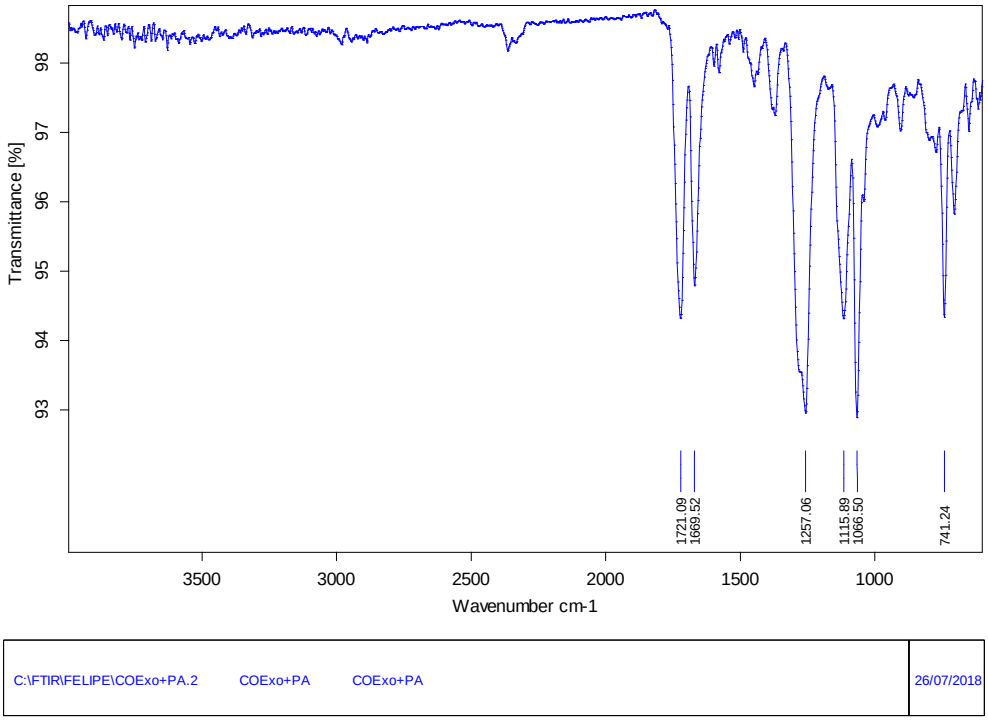

Figure S15. IR spectrum of poly(PA-*alt*-COexo) (**3**)

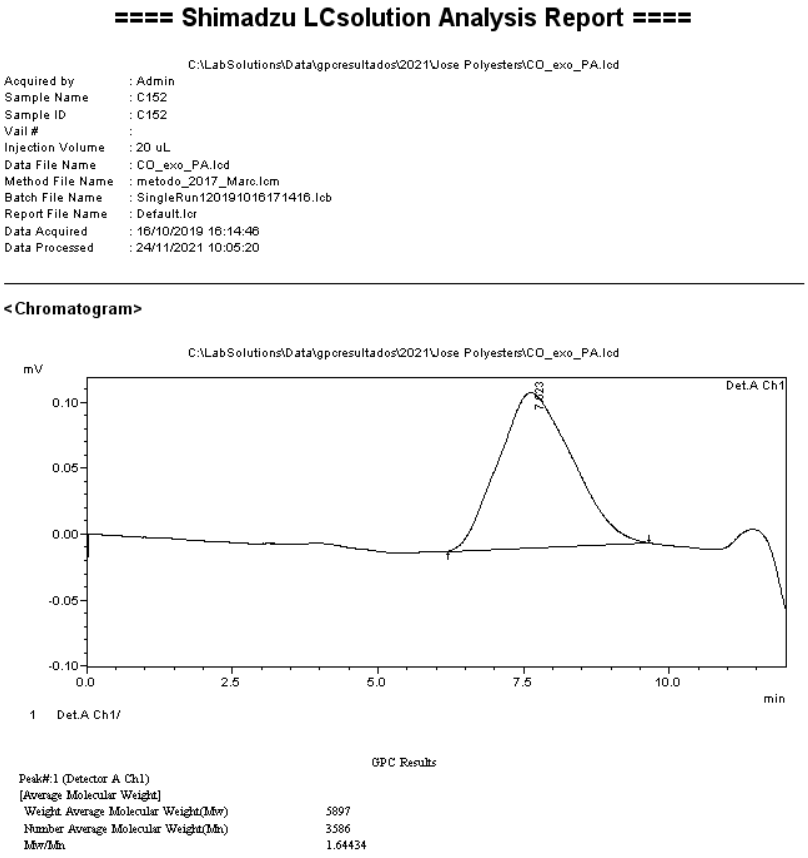

Figure S16. GPC profile of poly(PA-*alt*-COexo) (**3**)

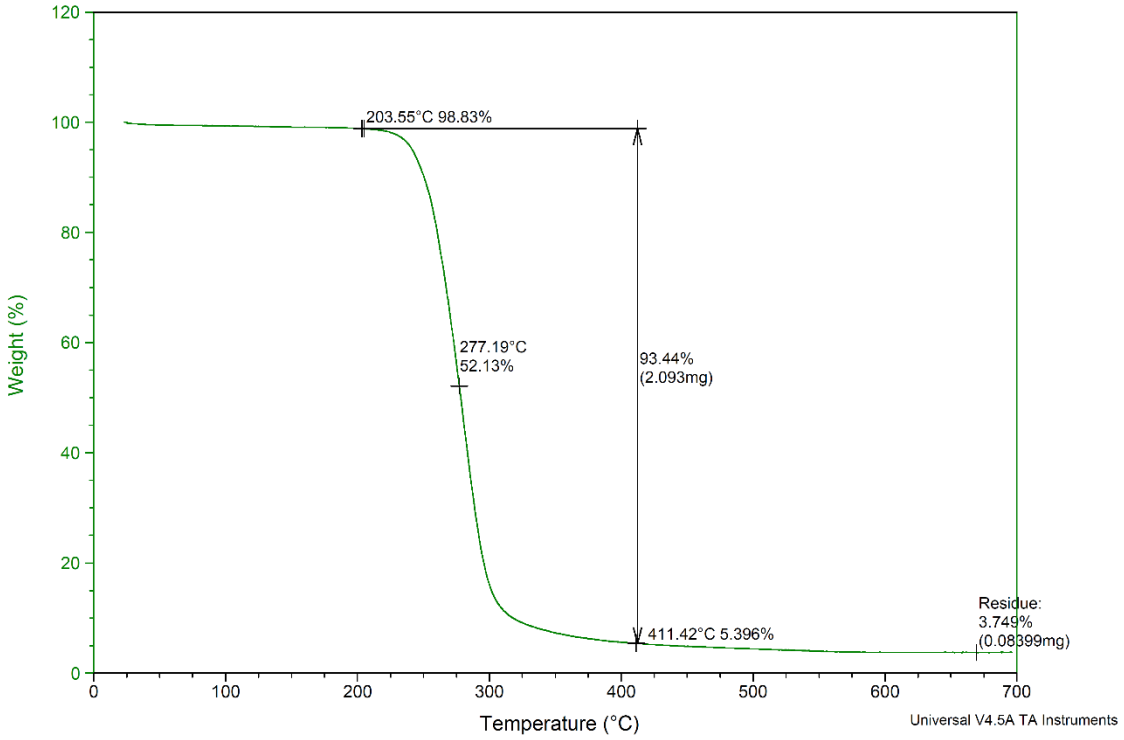

Figure S17. TGA analysis of poly(PA-*alt*-COexo) (**3**)

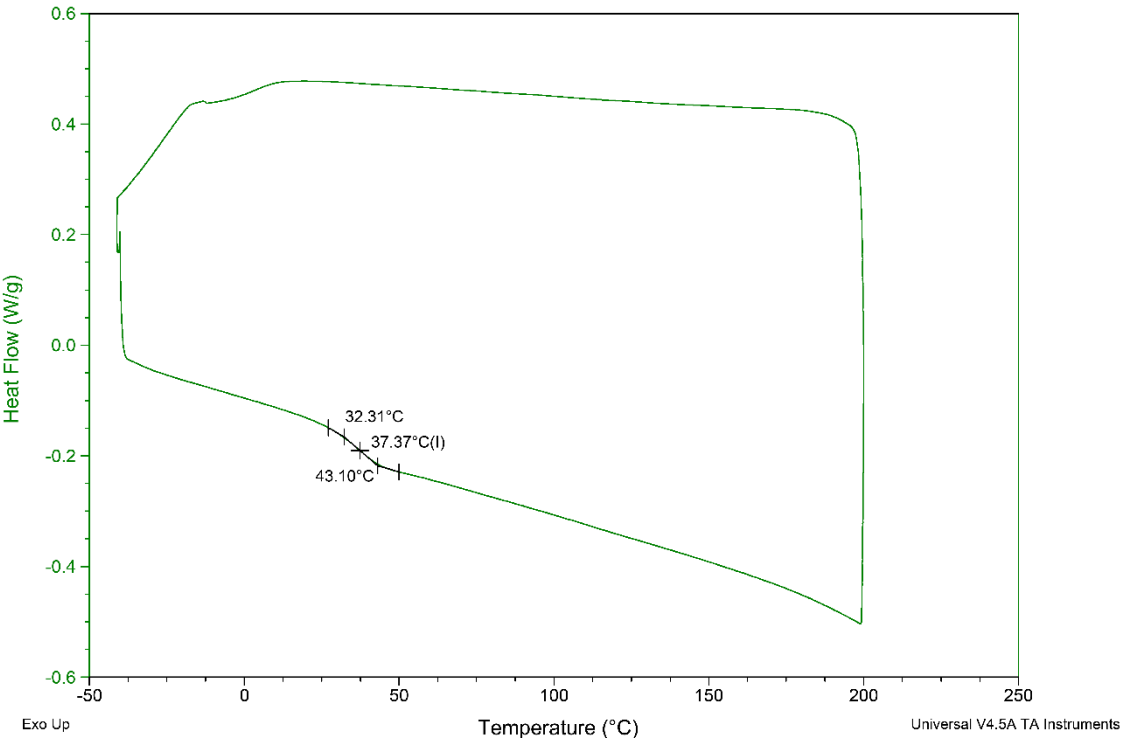

Figure S18. DSC analysis of poly(PA-*alt*-COexo) (**3**)

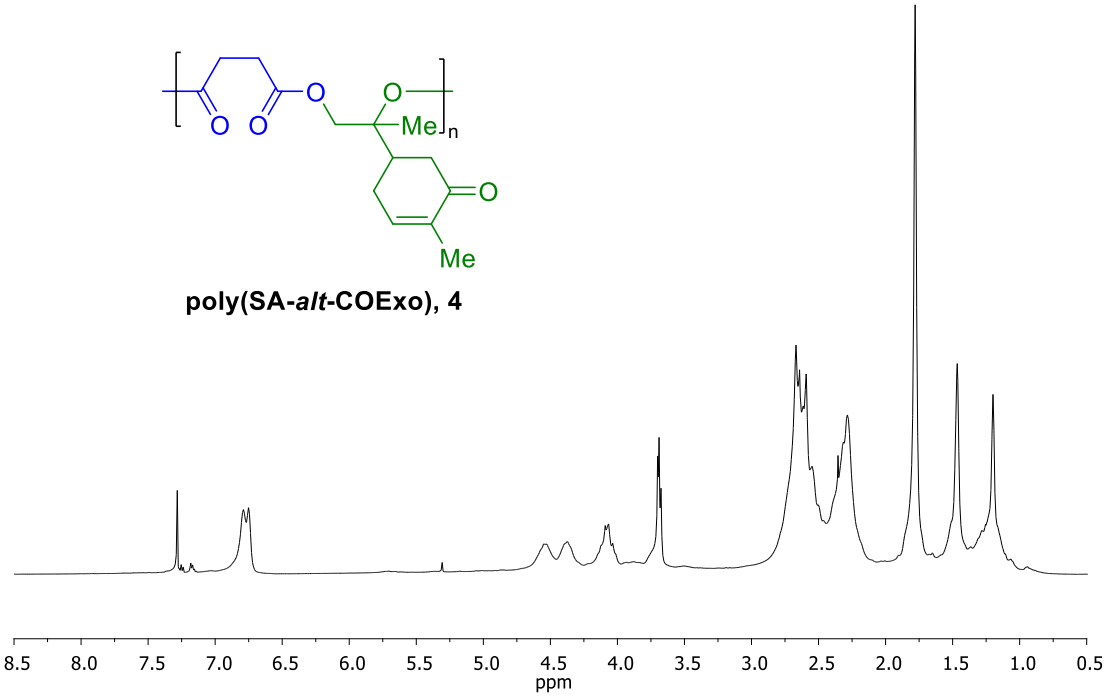

Figure S19. ^{1}H NMR spectrum of poly(SA-*alt*-COexo) (**4**)

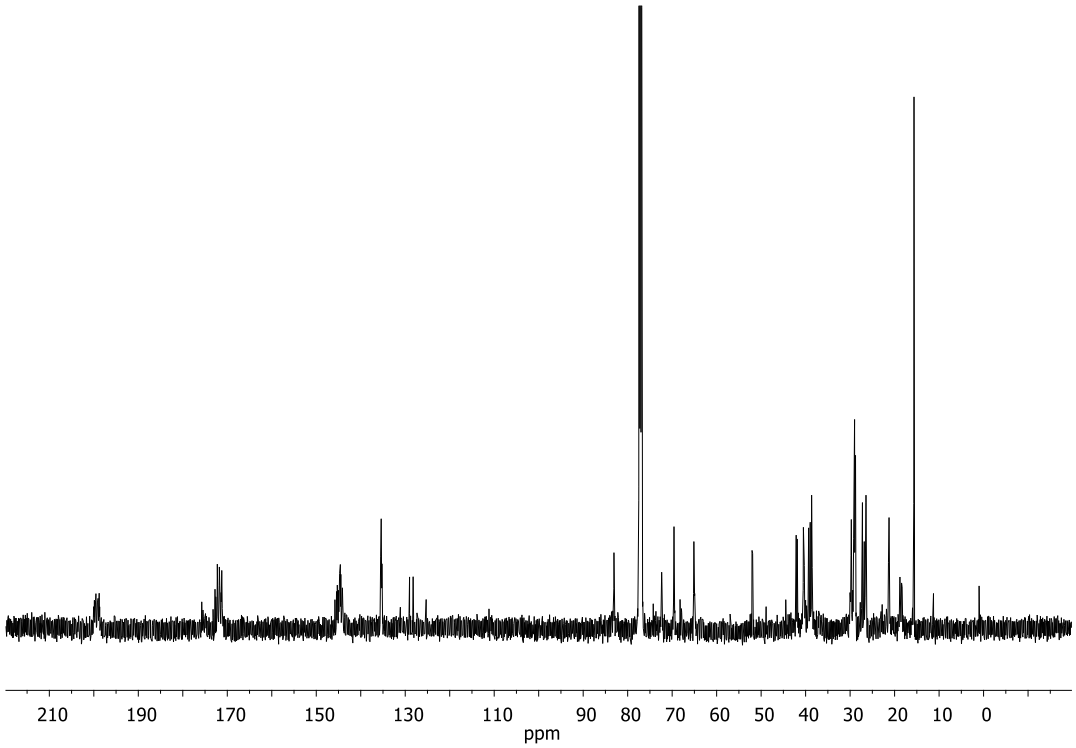

Figure S20. ^{13}C{^{1}H} NMR spectrum of poly(SA-*alt*-COexo) (**4**)

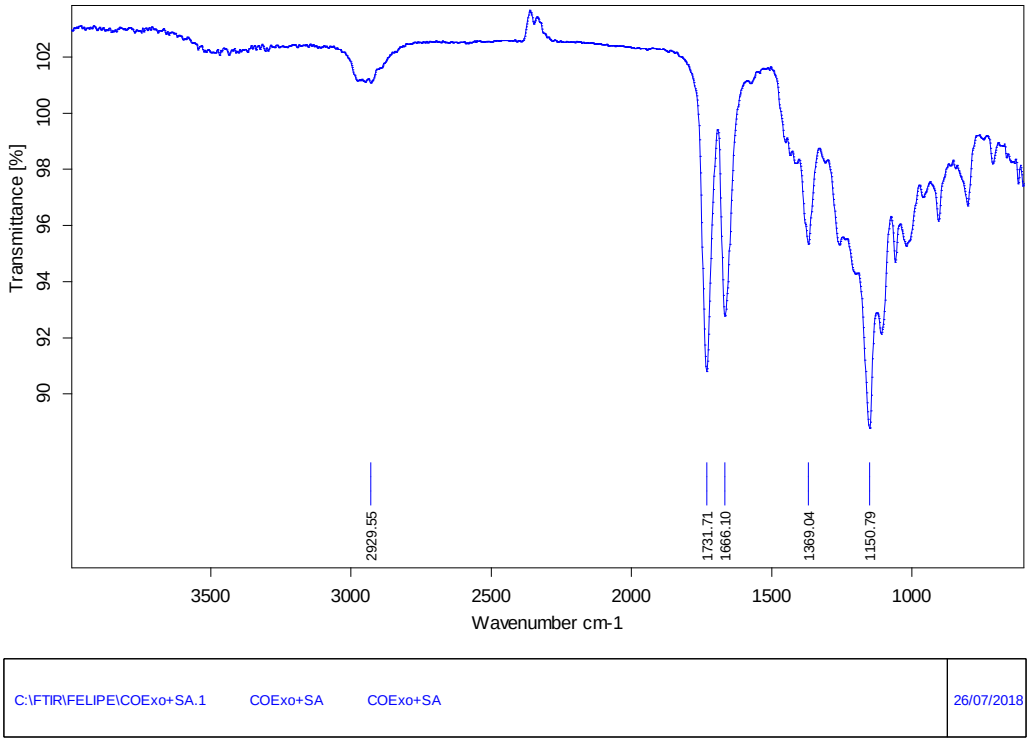

Figure S21. IR spectrum of poly(SA-*alt*-COexo) (**4**)

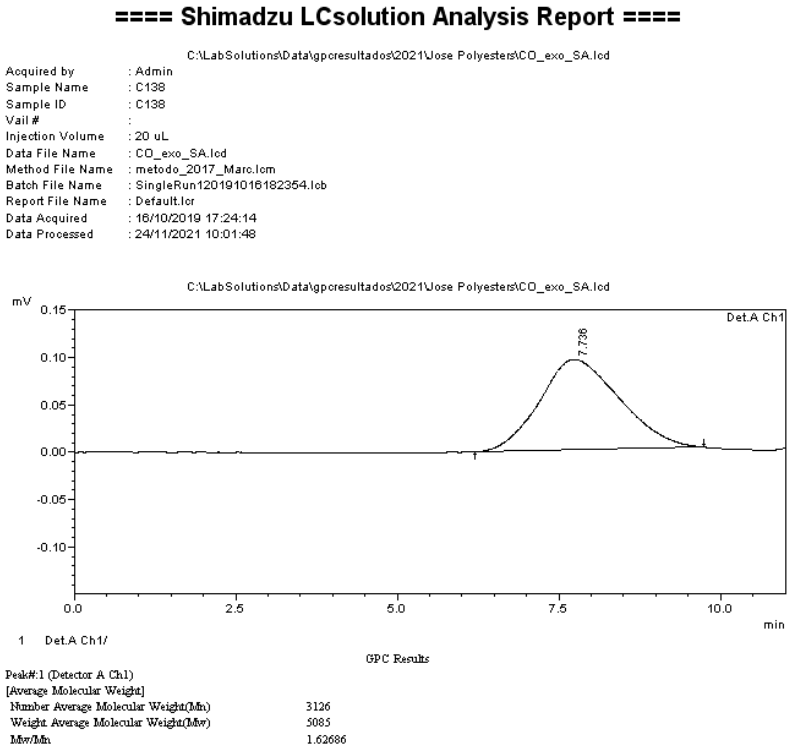

Figure S22. GPC profile of poly(SA-*alt*-COexo) (**4**)

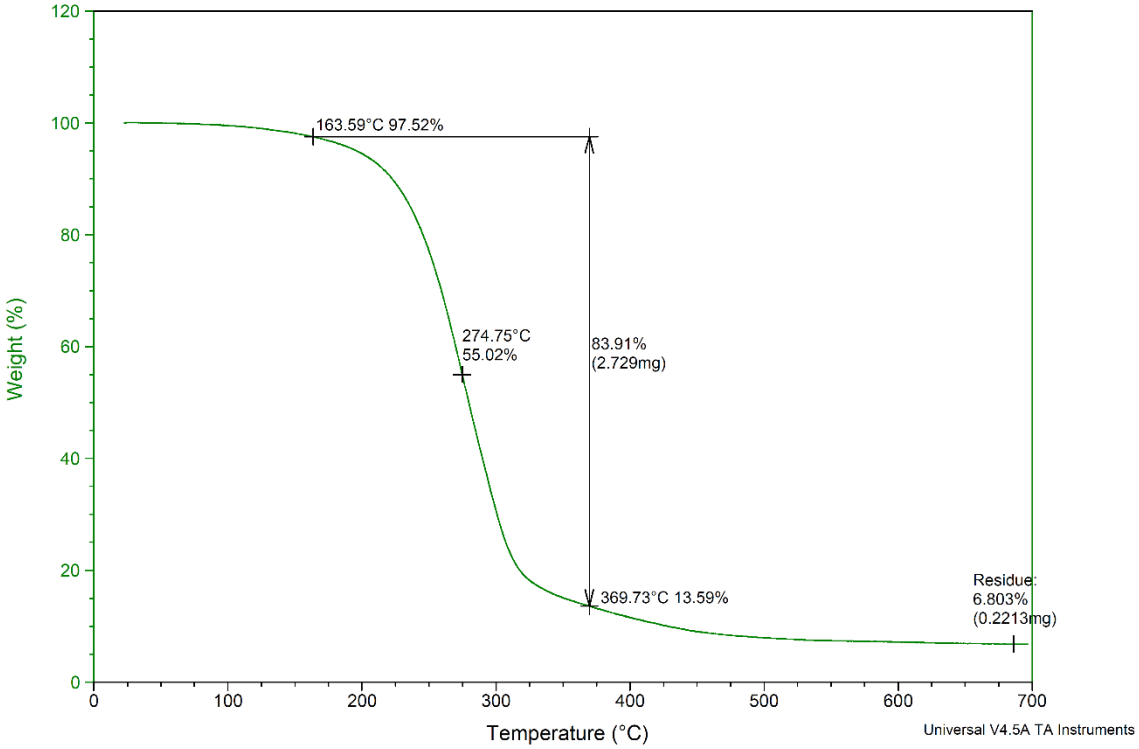

Figure S23. TGA analysis of poly(SA-*alt*-COexo) (**4**)

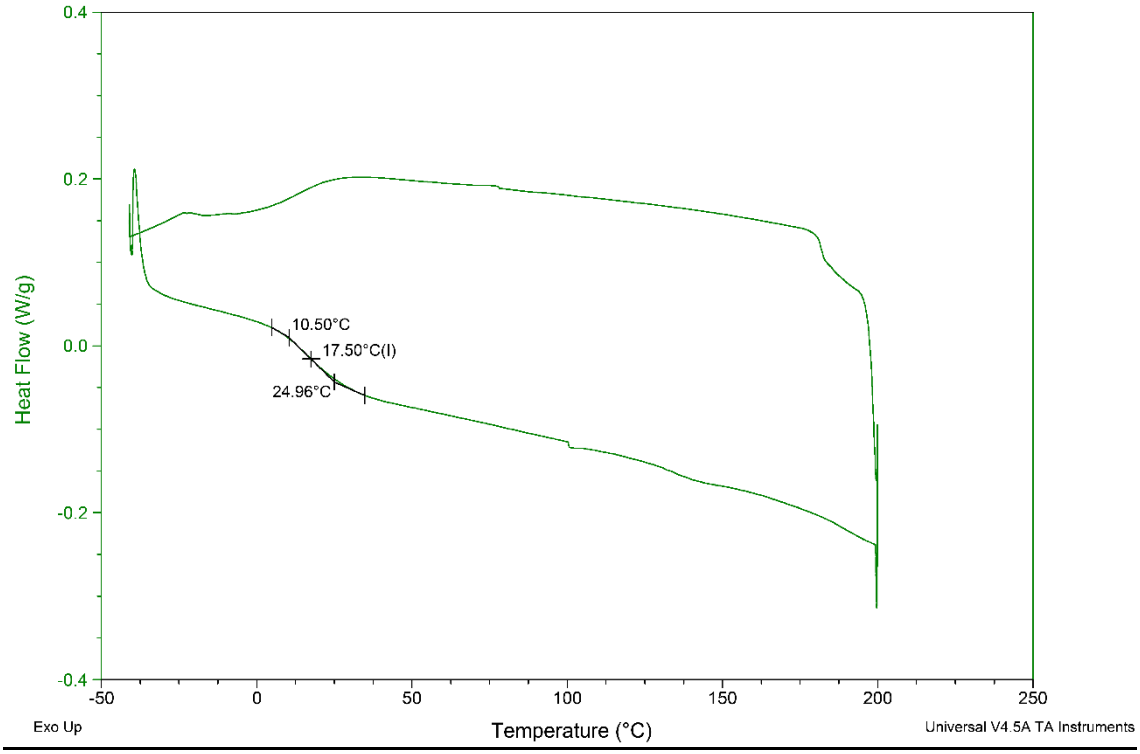

Figure S24. DSC analysis of poly(SA-*alt*-COexo) (**4**)

Table S2. Spectroscopic and Temperature Analysis values for each polymer in different environments at the same concentration (10^{-4} M)

Solvent	Sample	λ_{em} / nm (λ_{exc} =360 nm)	FWHM / cm^{-1}	S_r (30 ºC) / $ºC^{-1}$	T_m / ºC
TOL	1	424	6450	8.6	6.8
	2	431	7220	10.0	2.5
	3	434	7460	8.7	2.5
	4	438	7970	8.5	8.5
DMSO	1	466	7547	10.4	4.9
	2	461	7300	8.7	2.2
	3	485	8525	8.3	2.2
	4	467	6270	10.3	10.1
EtOH	1	460	5405	6.0	3.6
	2	446	7046	6.0	1.9
	3	436	7174	5.60	1.9
	4	465	6300	5.5	5.5
THF/H_2O (20%/ 80%)	1	396	4220	5.5	5.5
	2	395	4465	5.5	3.2
	3	396	5225	5.5	3.1
	4	450	6700	6.89	6.8
Solid	1	493	6630	7.8	4.6
	2	524	8570	10.4	3.9
	3	489	6545	12.2	3.5
	4	663	8100	14.4	2.5

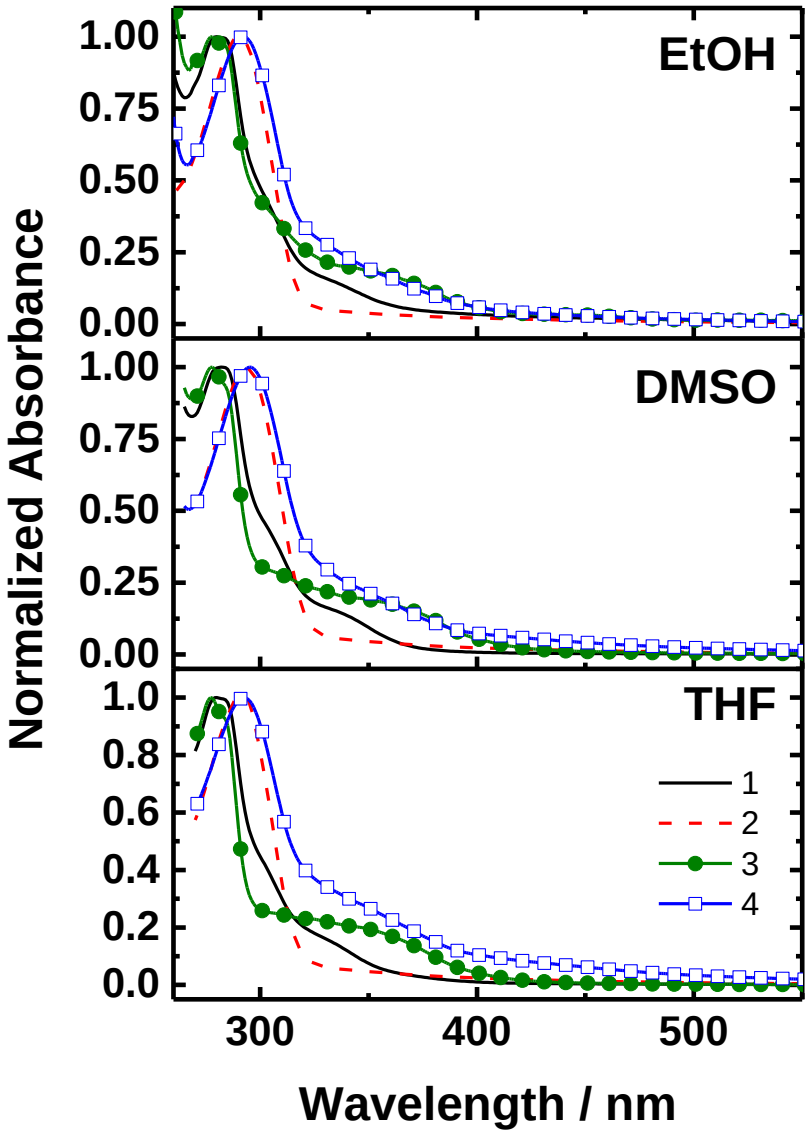

Figure S25. UV-visible spectra of polymers **1**-**4** at 10^{-4} M in different solvents.

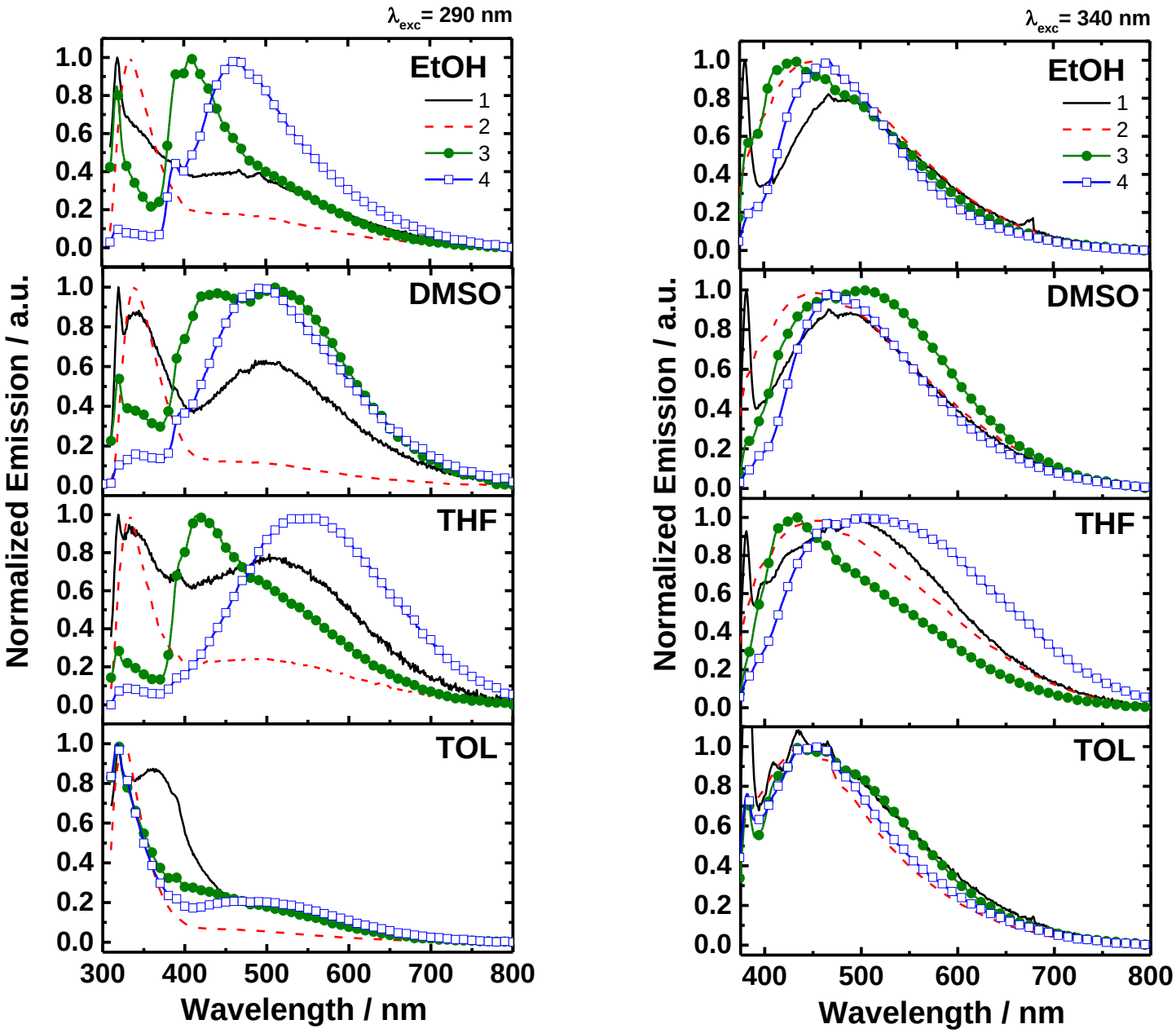

Figure S26. Emission spectra of polymers **1-4** at 10^{-4} M in different solvents upon excitation at **A)** 290 nm and **B)** 340 nm.

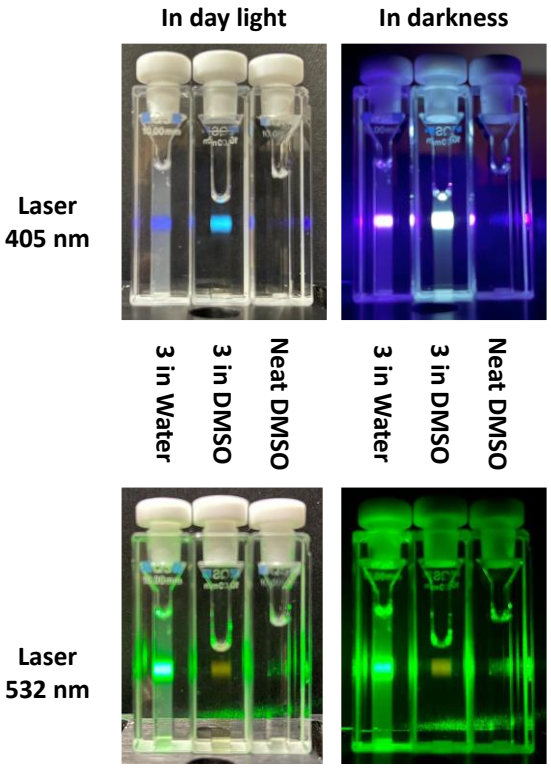

Figure S27: Photographic images of polymer 3 ($1x10^{-4}$ M) dissolved in water, DMSO in daylight (left) and in the darkness (right) upon irradiation at violet (405 nm; top) and green light laser (532 nm; bottom).

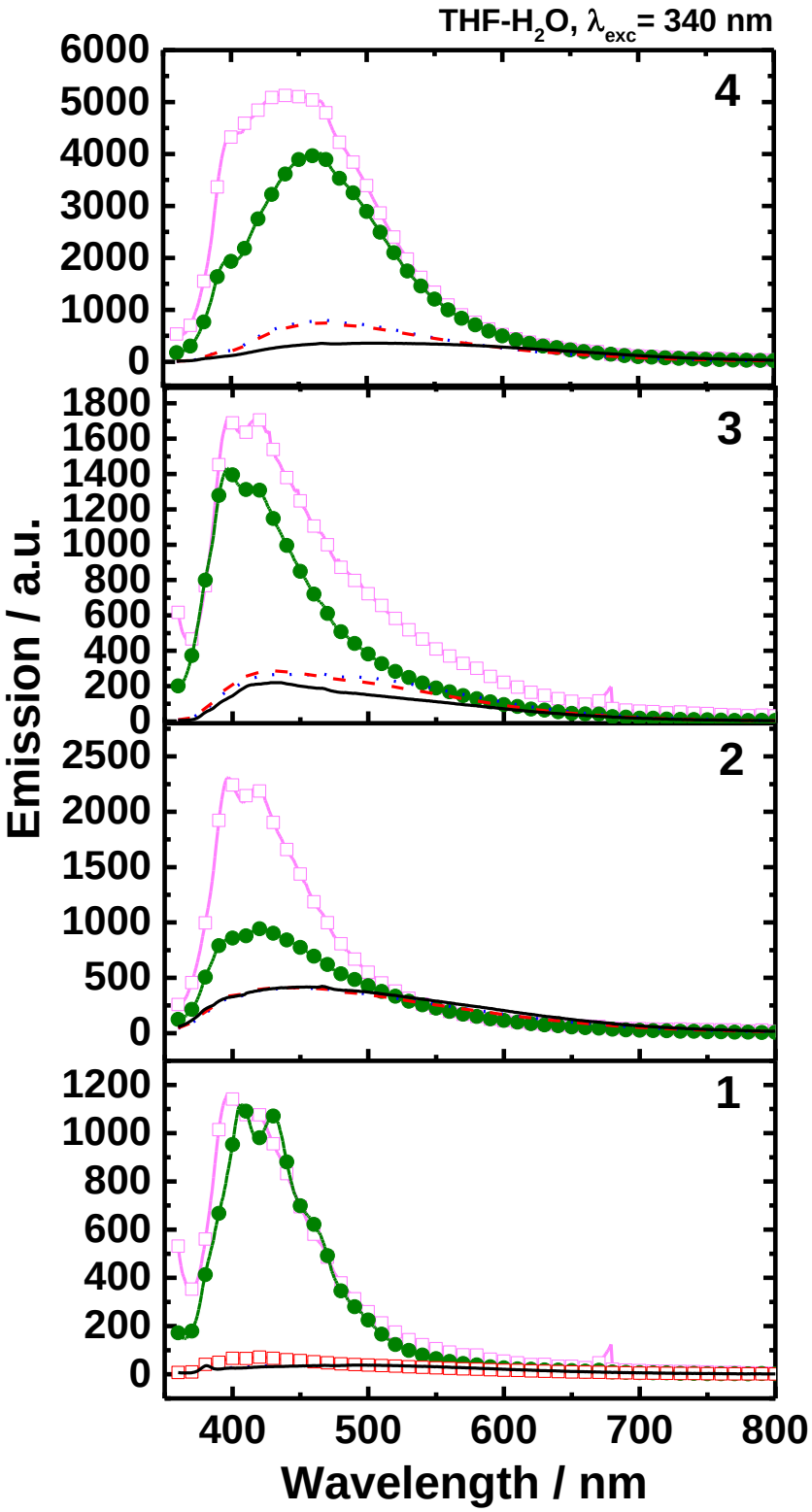

Figure S28. Emission spectra of polymers **1**-**4** in THF/H_2O mixtures from 0 (black line) to 80% wt water fraction.

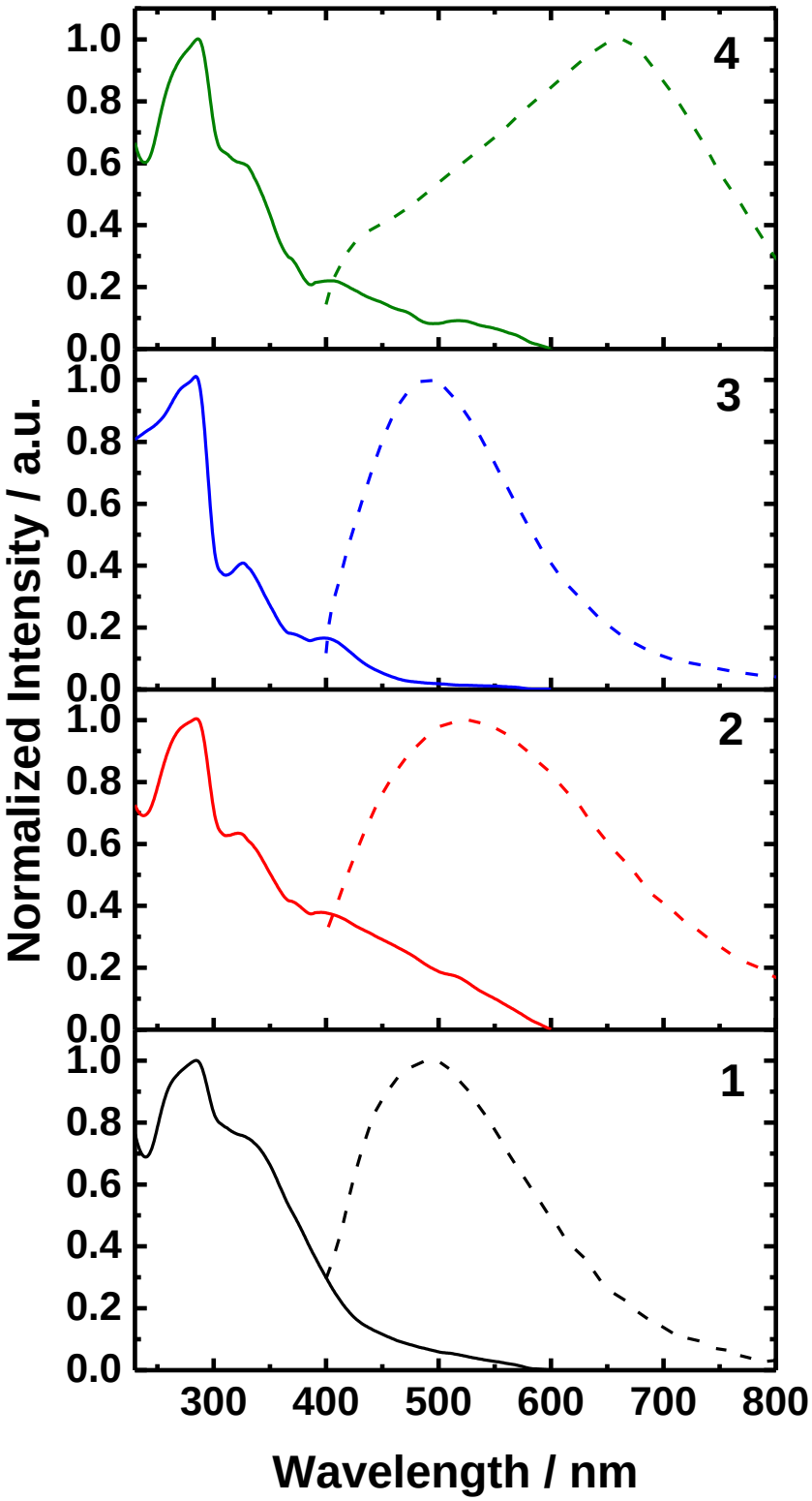

Figure S29. UV-visible spectra (solid line) and emission spectra (dashed line) upon excitation at 360 nm of polymers **1** (black), **2** (red), **3**(blue) and **4** (green), all the in solid state.

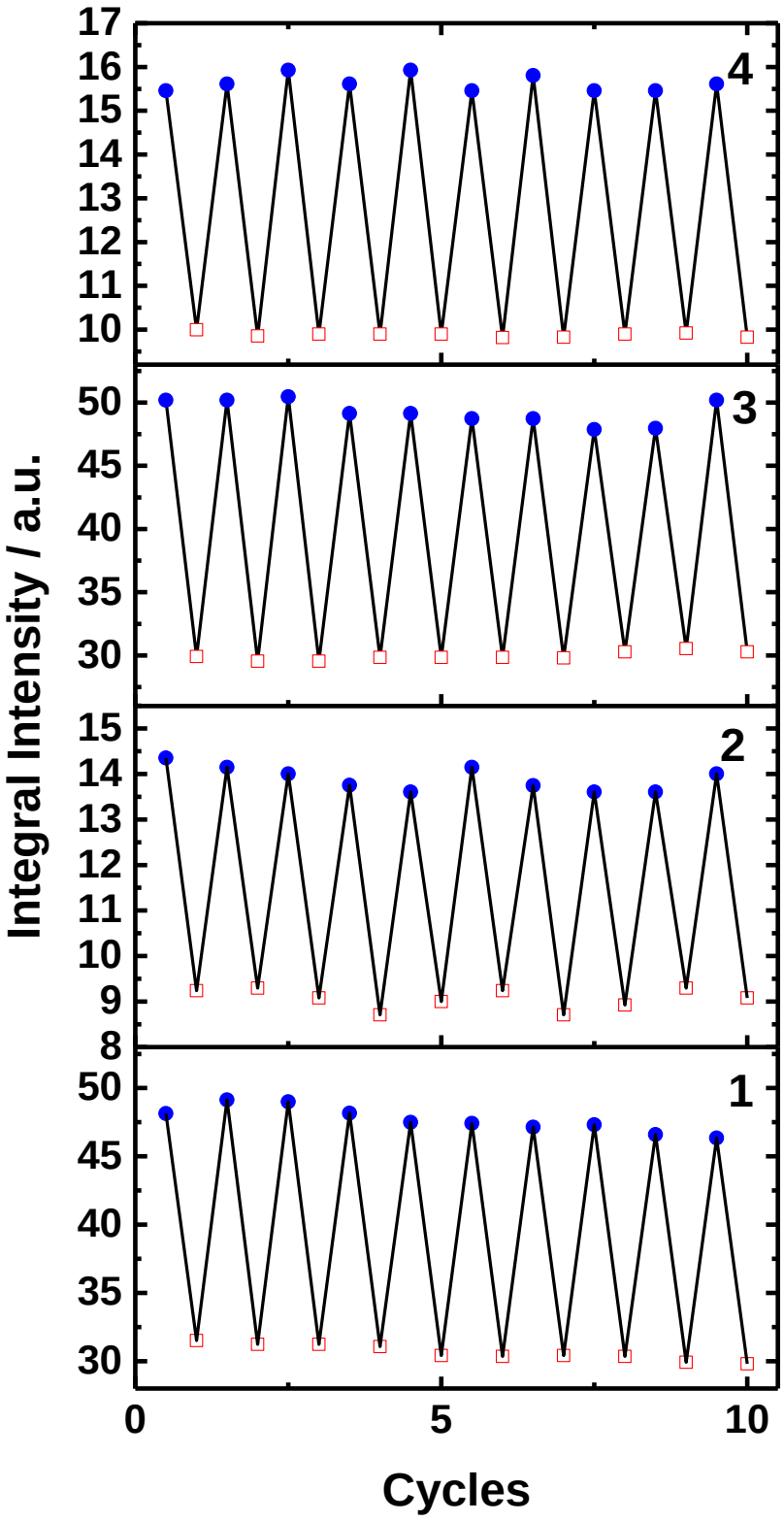

Figure S30. Integrated emission intensity (by calculating the area under the spectra) of each polymer recorded at 20°C and 100 °C subjected to 10 repeated heating-cooling cycles in solid state.

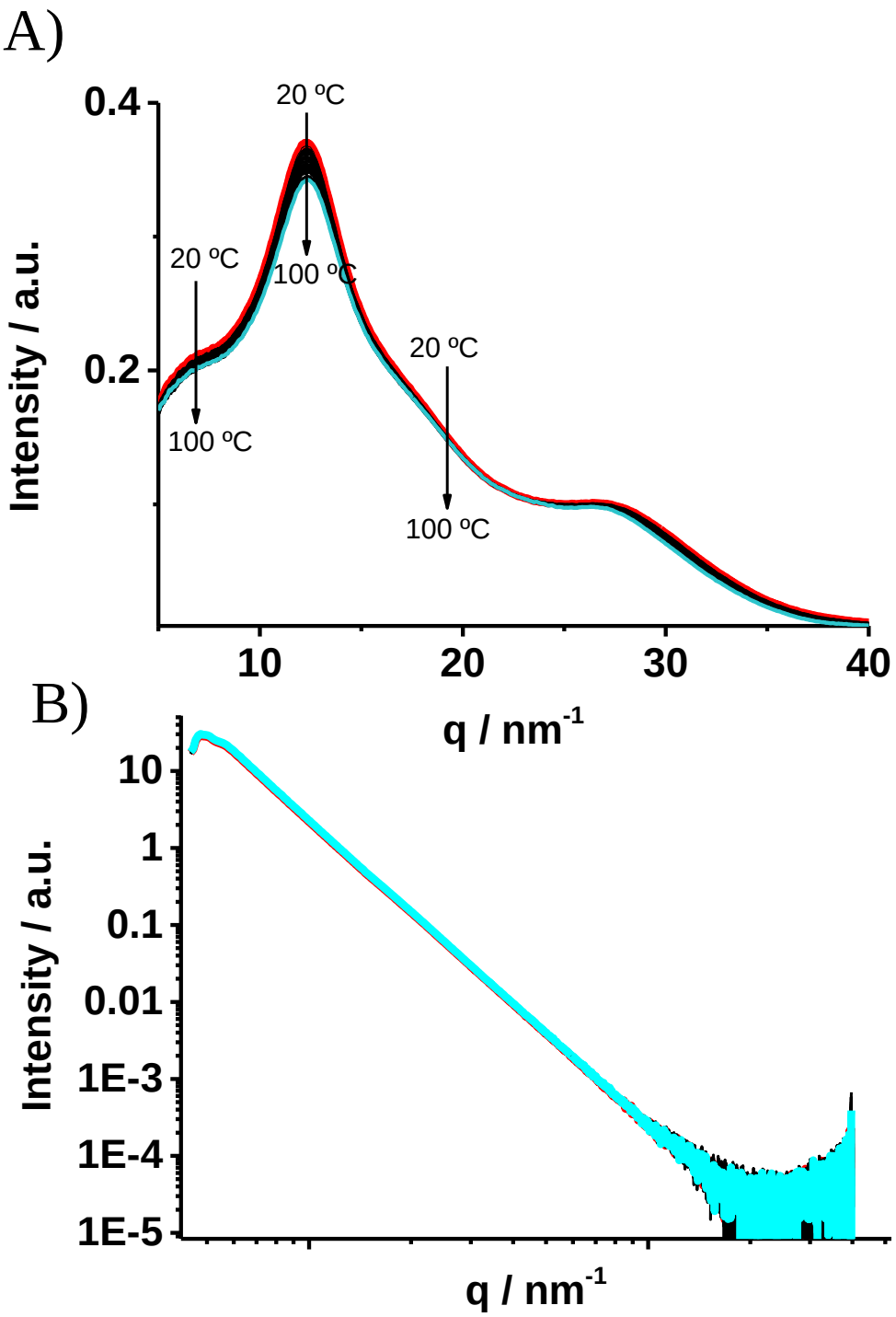

Figure S31. Dependence of **A)** WAXS and **B)** SAXS profiles of polymer 3 in solid state.

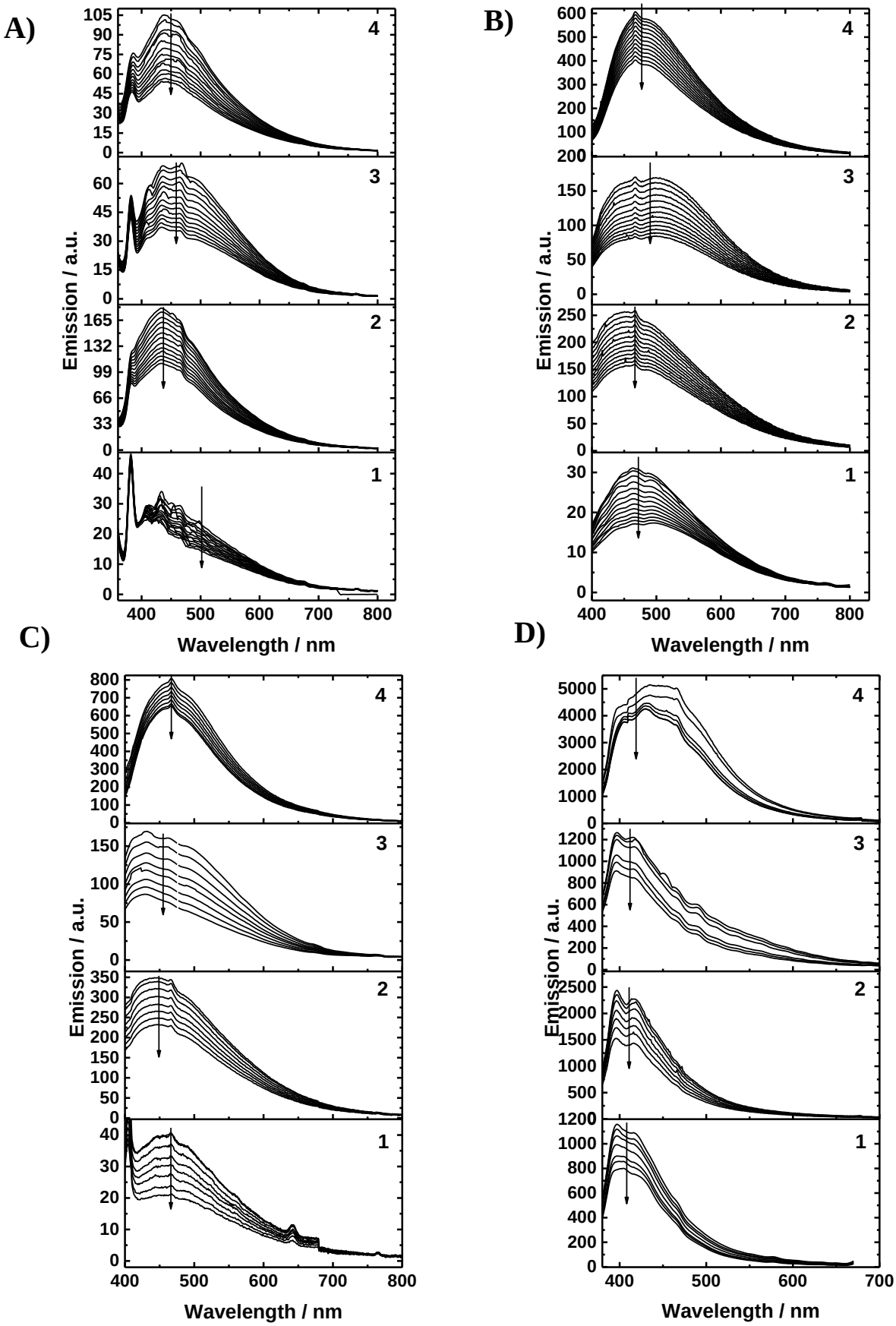

Figure S32. Emission spectra upon excitation at 360 nm of each polymer in **A)** TOL, **B)** DMSO, **C)** EtOH and **D)** THF-WATER solution as a function of temperature (10 - 80ºC).

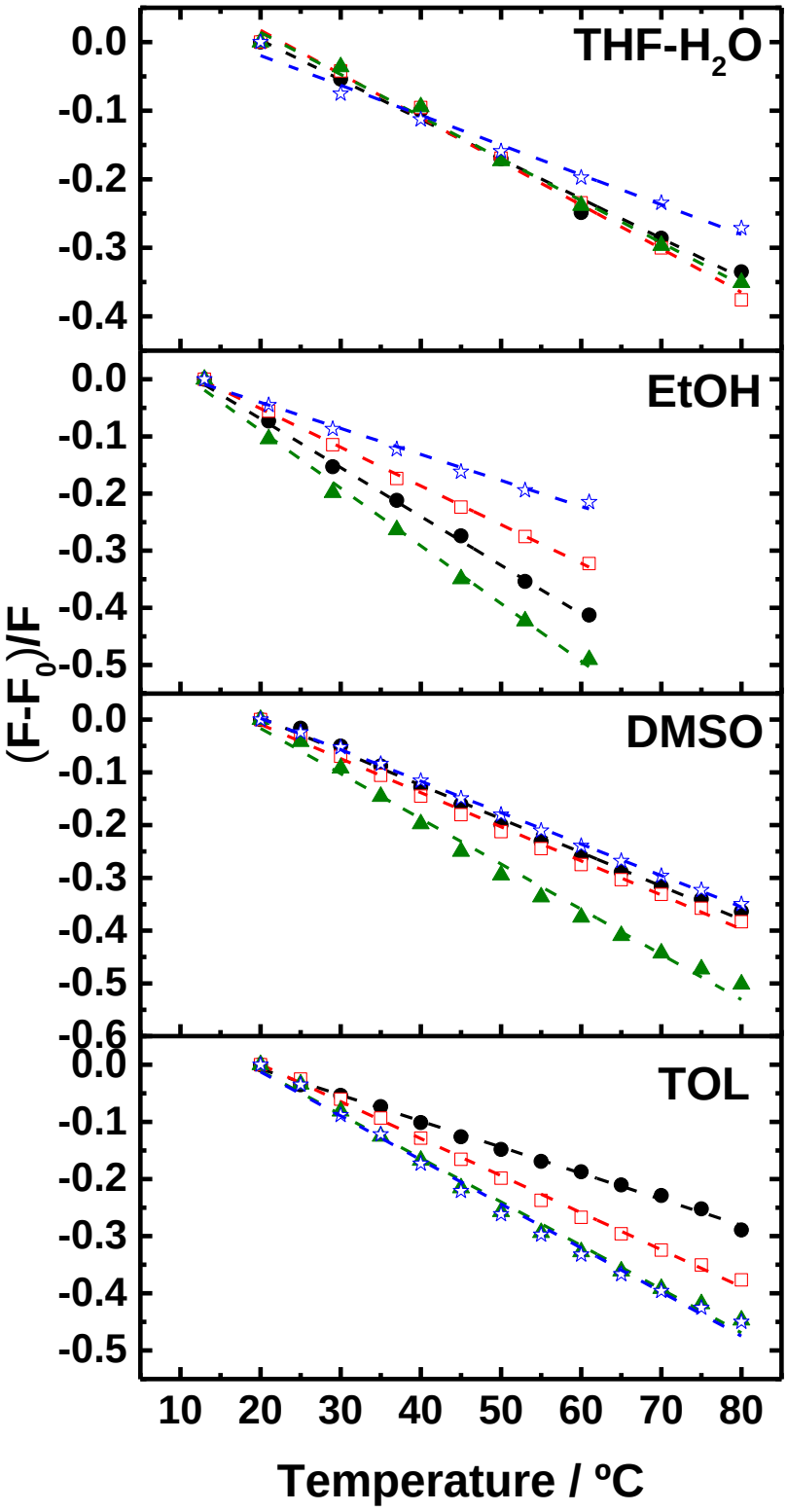

Figure S33. Correlation between change in intensity (F-F_0)/F vs sample temperature, showing a linear response in all polymers and solvents.

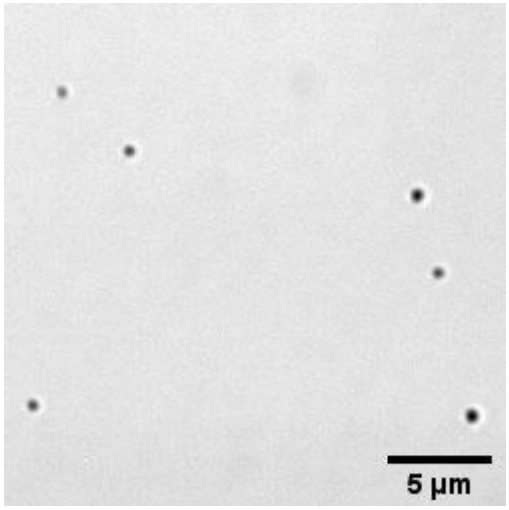

Figure S34. A representative transmission image of the Au NPs dropped cast onto the coverslip surface.